# Derivation of an Interatomic Potential for Fluoride-Containing Microporous Silicates and Germanates

German Sastre*,† and Julian D. Gale‡

*Instituto de Tecnologia Quimica U.P.V.-C.S.I.C, Universidad Politecnica de Valencia, Avenida Los Naranjos s/n, 46022 Valencia, Spain, and Nanochemistry Research Institute, Department of Applied Chemistry, Curtin University of Technology, P.O. Box U 1987, Perth 6845, Western Australia*

*Received September 15, 2004. Revised Manuscript Received November 22, 2004*

A new interatomic potential for simulating the properties of zeolites synthesized through the fluoride route has been derived. Hexafluoro compounds have been used as a basis for deriving a force field for the interaction of Si/Ge/Al ions with fluoride ions, as a starting point for describing the chemical behavior of the fluoride anions in the cavities of zeolites. From this, as well as ab initio data concerning the interaction of fluoride with framework, the equilibrium location of $F^-$ in the different small cavity environments found in zeolites can be calculated. It is found that the pentacoordination of Si due to formation of Si−F bonds is predicted by our model. The calculated Si−F distances for each case are found to be in excellent agreement with recent $^{19}F$ NMR and single-crystal XRD results. Furthermore, our force field can be used to predict distances in any zeolite, and in particular to establish the effect of Ge−F interactions and the corresponding equilibrium distances, which in some cases are not yet available experimentally. This new force field can be used in zeolites containing any compositional range with Si/Ge/Al as framework atoms, in the presence or absence of fluoride. Aluminogermanates and silicoaluminogermanates can therefore also be studied and the results used as a guide for new synthesis experiments using the fluoride route.

## 1. Introduction

The use of fluoride in the synthesis of zeolites, first introduced by Flanigen and Patton,[1] has allowed new structures to be obtained due to the special role played by this anion during the synthesis. The fluoride influences the process in at least two ways. First, it acts as a mineralizing agent that increases the solubility of silica species at neutral pH. Second, it functions as a catalyst in the condensation reactions that lead to the formation of Si−O−Si bonds.[2,3] An additional effect of $F^-$ as a structure directing agent has also been claimed because it tends to favor small cavities, in particular those containing at least one four-membered ring (MR) and, if the synthesis is carried out in germania-forming media, toward double four ring (D4R) cavities. Zeolites obtained by this route tend to be low-density materials, with few framework defects and large crystallite sizes.[4] Furthermore, materials with nonlinear optical properties are often found as products, such as [F-BQ]-IFR.[5]

Fluoride anions tend to be located inside small cavities of the zeolite, and in particular near 4-MR, where they are believed to form stable intermediates during the synthesis process.[3] Although the electrostatic repulsion between $F^-$ and the framework oxygens in a small cavity is an impediment to $F^-$ stabilization inside such regions, other factors, related to both electrostatic and short-range interactions combine to provide an overall stabilization of $F^-$ in small cages. The trend of fluoride anions to locate themselves in small cages of zeolites points to a different mechanism for the silica condensation reactions from that observed in $OH^-$-containing media, and so a mechanism involving either trigonal bipyramid species (pentacoordinated $[SiO_{4/2}F]^-$) or fluoride bridging the condensing silicate species is proposed.[6] The way in which charge is balanced in $OH^-$ and $F^-$ systems is essentially different, and while in the case of the former anion connectivity defects give rise to terminal silanol groups, the latter leads to extraframework fluoride anions located in the intracavity space available within the material. The $F^-$ ion is subjected to varying environments in different zeolites, and in all cases a tendency to coordinate to Si atoms is observed.[5,7−10] Five- and six-fold coordinated Si compounds

* To whom correspondence should be addressed. E-mail: gsastre@itq.upv.es.
† Universidad Politecnica de Valencia.
‡ Curtin University of Technology.

(1) Flanigen, E. M.; Patton, R. L. U.S. Patent 4,073,865, 1978.
(2) Guth, J. L.; Kessler, H.; Wey, R. In *New Developments in Zeolite Science and Technology, Proceedings of the 7th International Zeolite Conference*; Murakami, Y., Ijima, A., Ward, J. W., Eds.; Elsevier: Amsterdam, The Netherlands, 1986; p 121.
(3) Guth, J. L.; Kessler, H.; Caullet, P.; Hazm, J.; Merrouche, A.; Patarin, J. In *Proceedings of the 9th International Zeolite Conference*; von Ballmoos, R., Higgins, J. B., Treacy, M. M. J., Eds.; Butterworth-Heinemann: Stoneham, MA, 1993; vol 1, p 215.
(4) Barrett, P. A.; Boix, E. T.; Camblor, M. A.; Corma, A.; Diaz-Cabañas, M. J.; Valencia, S.; Villaescusa, L. A. In *Proceedings of the 12th International Zeolite Conference*; Treacy, M. M. J., Marcus, B., Higgins, J. B., Bisher, M. E., Eds.; Materials Research Society: Warrendale, PA, 1999; p 1495.
(5) Bull, I.; Villaescusa, L. A.; Teat, S. J.; Camblor, M. A.; Wright, P. A.; Lightfoot, P.; Morris, R. E. *J. Am. Chem. Soc.* **2000**, *122*, 7128.
(6) Barrett, P. A.; Camblor, M. A.; Corma, A.; Jones, R. H.; Villaescusa, L. A. *J. Phys. Chem. B* **1998**, *102*, 4147.
(7) Fyfe, C. A.; Brouwer, D. H.; Lewis, A. R.; Chezeau, J. M. *J. Am. Chem. Soc.* **2001**, *123*, 6882,
(8) van de Goor, G.; Freyhardt, C. C.; Behrens, P. *Z. Anorg. Allg. Chem.* **1995**, *621*, 311.

10.1021/cm048406o CCC: $30.25 
Published on Web 01/19/2005

have been known for a long time[11] and, in particular, hexafluoro compounds (i.e., $Na_2SiF_6$) demonstrate the ability of Si to coordinate octahedrally by forming six Si−F bonds.

The precise length of typical Si−F distances in zeolites is open to debate, since generally they are reported from single-crystal XRD measurements[5,9,10] whose local structure, as a result of the $F^-$ cage occupation being lower than 100%, is normally averaged over occupied $[SiO_{4/2}F]^-$ and unoccupied $[SiO_{4/2}]$ cages, which yields Si−F distances larger than the real ones. Values usually fall in the range 1.85−2.10 Å. For example, Si−F distances of 1.87, 1.92, and 2.08 Å are reported in STF,[10] IFR,[10] and MFI,[7] respectively. For the local structure of the pentacoordinated Si, two longer bond distances are found for Si−F and its opposing Si−O bond, whereas the other three Si−O bonds in the equatorial plane of the trigonal bipyramid are somewhat shorter. In addition, $O_{eq}-Si-O_{ax}$ angles near 90° are reported,[10] and they have also been found in ab initio calculations.[12] In comparison, Si−O bond distances in stishovite are between 1.76 and 1.81 Å.[13] Static and/or dynamic disorder may also add to the difficulty of identifying the exact $F^-$ location. Static disorder appears when multiple stable $F^-$ minima positions are found inside the cavity, and dynamic disorder appears when hopping between minima positions is observed at a given temperature. Using XRD, static disorder has been found to exist in SSZ-23[9] and SSZ-35,[10] whereas dynamic disorder has been observed by $^{19}F$ NMR in ITQ-4.[10]

Fluoride ions may also reside in close proximity to the positively charged structure-directing agent (SDA) as an ion pair (this result is subject to some controversy) in the main void volume of the zeolite,[14] although the location in a small cavity seems more probable.[15] In all the other cases, $F^-$ ions are reported to occupy small cages such as $[4^15^46^2]$ in NON, $[4^35^4]$ in SSZ-23, $[4^35^26^1]$ in ITQ-4, and $[4^15^26^2]$ in ZSM-5, SSZ-35, and SSZ-44.

Computer simulation has the potential to be a valuable tool in the study of fluoride-containing systems. For instance, it would be possible to characterize the locations of $F^-$ in different zeolite cavities, via the Si−F distances for a single configuration, and the dynamics within the cavities, through the possibility of simulating the hopping of the anion between sites of similar energy. Furthermore, it creates the possibility of studying the effect of the chemical composition on Si−F distances, stability, and dynamics, which may have a predictive, as well as a complementary, value to experiments. For example, the $F^-$ location in pure germania zeolites is, to date, only available for structures with a D4R ($[4^6]$ cavity)[16] as the cage in which the anion is situated. Hence, it would be interesting to know the location and energetics of $F^-$ in $GeO_2$ cavities such as $[4^15^46^2]$, $[4^35^4]$, $[4^35^26^1]$, or $[4^15^26^2]$, to name but a few alternative states. Similarly, it would be of interest to simulate zeolites with different Si/Ge contents, and to study the effect of introducing Al into the framework composition, for example in Si/Al, Si, Al/Ge, and Al/Ge zeolites. The fluoride synthesis route is important, not only as a pathway for creating new materials with no connectivity defects, but also as a valid route to incorporate Al or Ti into zeolite frameworks.[17] Pure silica structures are interesting for their hydrophobic properties, which have found application in selective adsorption, as well as the synthesis of materials with anchored organosilicon compounds with catalytic applications.[18]

To make all the above feasible, a reliable and consistent force field is required for microporous solids containing Si, Ge, and Al within the framework and $F^-$ as the counterion. To derive such a comprehensive potential model is the aim of this work.

## 2. Methodology

Our strategy here is to define a force field for the Si/Ge/Al/O/F system based on the Born model of ionic solids. The parameters of the potentials contained within the model are to be determined through empirical fitting to a large body of experimental data. It might be argued that this approach is restricted by the very ambiguities in the experimental information that we are trying to resolve. However, by employing physically motivated functional forms, and concurrently fitting to multiple structures and physical quantities, it is possible to obtain a satisfactory mean fit. Indeed, this process is capable of identifying inconsistent data within the training set.

**2.1 Potential Fitting.** Empirical fitting consists of minimizing the difference between observed and calculated properties by means of a least squares procedure. Concurrent fitting of multiple structures is found to enhance greatly the reliability of the derived potentials and generally leads to more physically reasonable potentials without the use of constraints. A fit must ideally be derived from chemical data as close as possible to the structures that will be subsequently modeled. In our case, as-synthesized $F^-$ zeolites have the inconvenience that they also contain, apart from the zeolite framework and the fluoride anion, an organic SDA that makes fitting difficult. This complication arises due to several factors, such as the difficulty in locating by XRD the coordinates of all the SDA atoms due to disorder. Furthermore, the presence of a large number of parameters, many of them coming from the intramolecular SDA interaction, adds to the complexity of the system and sometimes makes fitting intractable. Ideally, a good system for fitting must consist of a simple system with ordered and well-characterized atomic positions, with as few chemical components as possible. For this reason, we have chosen not a zeolite

(9) Camblor, M. A.; Diaz-Cabañas, M. J.; Perez-Pariente, J.; Teat, S. J.; Clegg, W.; Shannon, I. J.; Lightfoot, P.; Wright, P. A.; Morris, R. E. *Angew. Chem., Int. Ed.* **1998**, *37*, 2122.
(10) Villaescusa, L. A.; Wheatley, P. S.; Bull, I.; Lightfoot, P.; Morris, R. E. *J. Am. Chem. Soc.* **2001**, *123*, 8797.
(11) Liebau, F. *Structural Chemistry of Silicates*; Springer-Verlag: Berlin, 1985.
(12) Attfield, M. P.; Catlow, C. R. A.; Sokol, A. A. *Chem. Mater.* **2001**, *13*, 4708.
(13) Sinclair, W.; Ringwood, A. E. *Nature* **1978**, *272*, 714.
(14) Price, G. D:; Pluth, J. J.; Smith, J. V.; Bennett, J. M.; Patton, R. L. *J. Am. Chem. Soc.* **1982**, *104*, 5971.
(15) Mentzen, B. F.; Sacerdote-Peronnet, M.; Guth, J. L.; Kessler, H. *C. R. Acad. Sci. Paris* **1991**, *313*, 177.
(16) Li, H.; Yaghi, O. M. *J. Am. Chem. Soc.* **1998**, *120*, 10569.
(17) Camblor, M. A.; Villaescusa, L. A.; Díaz-Cabañas, M. J. *Top. Catal.* **1999**, *9*, 59.
(18) Jones, C. W.; Tsuji, K.; Davis, M. E. *Nature* **1998**, *393*, 52.

structure, but hexa-(Si,Al,Ge)-fluoride salts for the fit of the Si−F interaction. Within the scope of possible fluoride compounds, a valid alternative would have also been to use the corresponding binary tetrafluorides. However, the octahedral coordination of the hexafluorides was preferred to that found in the tetrahedral compounds because of its greater similarity to the environment in $F^-$ zeolites, where fluoride anions tend to change the tetrahedral coordination of the framework cation to a 5-fold configuration.

The structures of $Na_2SiF_6$,[19] $Na_2GeF_6$,[20] and $Na_3AlF_6$[21] have been well characterized by XRD and provide the data from which we can determine the Si−F, Ge−F, and Al−F interactions, as well as the F−F interaction. After this, the next step is to obtain reliable parameters for the O−F interactions which are present in $F^-$ zeolites, but not in the hexafluoro-compounds, and this can be obtained by a fit to known $F^-$ zeolite structures. The procedure involves optimizing a zeolite system (including $F^-$ and organic $SDA^+$) with a given set of O−F parameters, and then varying the O−F parameters searching for those which best reproduce the experimental structure. Because of the complexity of these materials, an initial manual refinement was performed, which means that the parameters were varied systematically searching the optimum values. Subsequently, a refinement of the O−F interaction was performed based on ab initio data for fluoride in a low-symmetry environment.

In a previous study[22] we derived a fit for Si/Ge zeolites, and in the present work we extend this fit to include Al substitution. For this purpose, we have chosen the well-characterized Na−LTA structure[23] with Si/Al = 1, and strict Si−Al alternation which, assuming that Lowenstein's rule[24] is obeyed, guarantees that the structure is ordered. An approach is taken that is similar to that of our previous study of Si/Ge zeolites[22] for the Al fit, and the oxygen polarizability is assumed to be the same as in silica structures, as explained below.

In the present work, the relaxed fitting scheme[25] is employed for the final refinement of the potential parameters, as implemented within the program GULP.[26,27] Here the structure of every phase is minimized at each point of the least-squares procedure and the displacements from the experimentally observed structure form the basis of the residuals, instead of just using the forces acting on the structure at the experimental geometry. Similarly, the curvature related properties are evaluated at the optimized structure since this is more reliable and formally correct.

When considering the hexafluoro-compounds the potential model is the Born model and consists of the Coulomb interaction, evaluated via an Ewald summation, and a short-range pair potential described by a Buckingham function with cutoff distance of 12 Å. The shell model was used to simulate the dipolar polarizability of the fluorine ions. The functional forms are as follows:

$$E^{hexafluoro-compound} = E^{Buckingham} + E^{threebody} + E^{core-shell} + E^{Coulombic} \quad (1)$$

$$E_{ij}^{Buckingham} = A_{ij} \exp\left(-\frac{r_{ij}}{\rho_{ij}}\right) - \frac{C_{ij}}{r_{ij}^6} \quad (2)$$

$$E_{ijk}^{threebody} = \frac{1}{2}k_{ijk}(\theta - \theta_0)^2 \quad (3)$$

$$E_{ij}^{core-shell} = \frac{1}{2}k_{ij}^{cs}r_{ij}^2 \quad (4)$$

$$E_{ij}^{Coulombic} = \frac{q_i q_j}{4\pi\epsilon_0 r_{ij}} \quad (5)$$

The Buckingham potential has been employed successfully in modeling the repulsive (exponential term) and the attractive dispersive ($r^{-6}$ term) forces, so as to treat the interatomic interactions in a physically reasonable way, both for short and medium range distances. A cutoff radius of 12 Å is applied to the nonelectrostatic two-body interactions. The core−shell term has been shown to be essential in order to reproduce the properties of many solids, and we have included this description for the fluoride anion whose polarizability has to be reproduced accurately in our model. The core−shell term consists of a harmonic spring, which describes the increasing interaction between the negative charge cloud and the positive core of the fluoride anion as their mutual separation increases. Note that the electrostatic interaction between a core and shell of the same particle is specifically excluded, such that the spring is the only force acting between them.

When fitting the O−F interaction to a zeolite structure, the potential model described in our previous study[22] for the silica zeolite ($SiO_2$ framework + $F^-$ + $SDA^+$) was chosen, and apart from the terms previously described, a three-body interaction between O−Si−O terms is included to account for the $sp^3$ hybridation character of the partially covalent Si−O bonds (eq 3), where the equilibrium angle is $\theta_0 = 109.47°$.

For the organic SDA component, we have used the same approach as in previous publications,[28−31] which is to utilize the force field of Oie et al[32] for the intramolecular SDA interactions and the Kiselev force field[33] for the intermolecular SDA−zeolite interactions. More details are given below.

In modeling oxide materials, the shell model for the oxygen atoms has proven essential in order to fit dielectric constants, phonons, and other characteristic properties, and

(19) Schaefer, G. F. *Z. Kristallogr.* **1986**, *175*, 269.
(20) Cipriani, C. *Rend. Soc. Miner. Ital.* **1958**, *11*, 58.
(21) Ross, K. C.; Mitchell, R. H.; Chakhmonradian, A. R. *J. Solid State Chem.* **2003**, *172*, 95.
(22) Sastre, G.; Gale, J. D. *Chem. Mater.* **2003**, *15*, 1788.
(23) Pluth, J. J.; Smith, J. V. *J. Am. Chem. Soc.* **1980**, *102*, 4704.
(24) Lowenstein, W. *Am. Miner.* **1954**, *39*, 92.
(25) Gale, J. D. *Philos. Mag. B* **1996**, *73*, 3.
(26) Gale, J. D. *J. Chem. Soc., Faraday Trans.* **1997**, *93*, 629.
(27) Gale, J. D.; Rohl, A. L. *Mol. Simul.* **2003**, *29*, 291.
(28) Sastre, G.; Fornes, V.; Corma, A. *J. Phys. Chem. B* **2002**, *106*, 701.
(29) Sastre, G.; Lewis, D. W.; Catlow, C. R. A. *J. Phys. Chem.* **1996**, *100*, 6722.
(30) Sastre, G.; Vidal-Moya, J. A.; Blasco, T.; Rius, J.; Jorda, J. L.; Navarro, M. T.; Rey, F.; Corma, A. *Angew. Chem., Int. Ed.* **2002**, *41*, 4722.
(31) Sastre, G.; Leiva, S.; Sabater, M. J.; Gimenez, I.; Rey, F.; Valencia, S.; Corma, A. *J. Phys. Chem. B* **2003**, *107*, 5432.
(32) Oie, T.; Maggiora, T. M.; Christoffersen, R. E.; Duchamp, D. J. *Int. J. Quantum Chem., Quantum Biol. Symp.* **1981**, *8*, 1.
(33) Kiselev, A. V.; Lopatkin, A. A.; Shulga, A. A. *Zeolites* **1985**, *5*, 261.

**Table 1. Atomic Charges for the Templates Used in the Synthesis of Octadecasil, ASU-9, SSZ-35, and SSZ-44, Which Are *N,N,N*-Trimethyl-tert-butylammonium (TMTBA), DABCO, DMABO, and DECDMP, Respectively, in Their Protonated Forms[a]**

| atom | $TMTBA^+$ | $DABCO-H^+$ | $DMABO^+$ | $DECDMP^+$ |
|---|---|---|---|---|
| N4 | −0.3840 | −0.3071 | −0.4000 | −0.3160 |
| N3 | | −0.5180 | | |
| C1 | −0.2725 | | −0.3340 | −0.3783 |
| C2 | | −0.0765 | −0.1700 | −0.1858 |
| C3 | 0.1210 | | −0.0300 | 0.0395 |
| H | 0.1610 | 0.1757 | 0.1600 | 0.1533 |

[a] DABCO is 1,4-diazabicyclo [2.2.2] octane, DMABO is *N,N*-dimethyl-6-azonium-1,3,3-trimethylbicyclo [3.2.1] octane, and DECDMP is *N,N*-diethyl-2,6-cis-dimethylpiperidine. N4 and N3 are quaternary and tertiary nitrogen; C1, C2, and C3 are primary, secondary, and tertiary carbon atoms, respectively.

so similar fluoride anions are best treated in the same way. This is because the polarization may also act to mimic covalency effects that would lead to lower effective ionic charges than the formal ones that are chosen in the present study and many previous ones.[34−37]

Obviously, the present fit is entirely compatible with the previous Si/Ge force field[22] and the new fit does not introduce any modification for the modeling of Si/Ge zeolites. The advantage of the new fit is the extension to zeolites containing fluoride anions, as well as any combination of Si/Al/Ge atoms within the zeolite framework. Of course, any organic SDA occluded in the zeolite micropore can also be treated. A consequence of the compatibility is that the oxygen atom parameters have been retained and no new types of oxygens appear when introducing Al into the framework. In our model, as well as in previous studies,[35] oxygens in Al−O bonds are equivalent to oxygens in Si−O bonds and this is due to the negligible change in the oxygen polarizability in aluminosilicates with respect to silicates.

**2.2 Energy Minimization.** Once the parametrization was completed, energy minimizations were performed to examine the ability of the force field to reproduce the structure and vibrations associated to $F^-$ of octadecasil,[38] and the structures of SSZ-35 and SSZ-44,[39] which were not included in the original fit. Apart from the zeolite force field already described, the terms including the template molecule and its interaction with the zeolite are also necessary when the experimental XRD structure has been solved for noncalcined materials. The total potential energy function is given as follows:

$$E^{total} = E^{zeolite} + E^{complex} + E^{zeolite-complex} + E^{complex-complex} \quad (6)$$

The term $E^{zeolite}$ has already been described in eqs 1−5 and the other remaining terms are as follows:

$$E^{complex} = E^{harmonic} + E^{threebody} + E^{torsion} + E^{Coulombic} \quad (7)$$

$$E^{zeolite-complex} = E^{Lennard-Jones} + E^{Coulombic} \quad (8)$$

$$E^{complex-complex} = E^{Lennard-Jones} + E^{Coulombic} \quad (9)$$

Three-body and Coulombic terms are described in eqs 3 and 5, and the other terms are as follows:

$$E_{ij}^{harmonic} = \frac{1}{2}k_{ij}^{h}(r_{ij} - r_{ij}^{0})^2 \quad (10)$$

$$E_{ijkl}^{torsion} = k_{ijkl}^{t}[1 + \cos(n\phi - \phi_0)] \quad (11)$$

$$E_{ij}^{Lennard-Jones} = \frac{B_{ij}^{LJ}}{r_{ij}^{12}} - \frac{C_{ij}^{LJ}}{r_{ij}^{6}} \quad (12)$$

The Lennard−Jones potential is used instead of the previously described Buckingham potential for the repulsive and dispersive forces. Here the difference between the two functional forms is the $r^{-12}$ term employed for the repulsive part instead of an exponential. The benefit of employing the Lennard−Jones potential is that it contains only a single parameter, which simplifies the derivation of parameters for systems where there is a paucity of accurate data against which to fit, as is the case for the interaction of SDA molecules. For the bonded interactions within a SDA molecule, the use of harmonic functional forms for local interactions is appropriate since only small distortions about the equilibrium geometry occur. Finally, the torsional term is accounted for by a classical description based on a periodic cosine function with three parameters taking into account the equilibrium dihedral ($\phi_0$), the periodicity ($n$), and the energy barrier between conformations ($k$).

As previously mentioned, the force field parameters are taken from the works of Kiselev et al[33] and Oie et al[32] for the template−zeolite and template−template interactions, respectively. The templates used in the synthesis of octadecasil, ASU-9, SSZ-35, and SSZ-44 are *N,N,N*-trimethyl-terc-butylammonium, DABCO, DMABO, and DECDMP, respectively. All of these template molecules are in their protonated forms. DABCO is 1,4-diazabicyclo [2.2.2] octane, DMABO is *N,N*-dimethyl-6-azonium-1,3,3-trimethylbicyclo [3.2.1] octane, and DECDMP is *N,N*-diethyl-2,6-dimethylpiperidine. To treat in a realistic way the electrostatics of the interaction between the template and the zeolite, and between template molecules, full optimizations of the charged templates have been carried out at the Hartree−Fock level with the 6-31G** basis set, using the program NWChem,[40] and the corresponding Mulliken charges extracted as listed in Table 1.

## 3. Results and Discussion

**3.1 Force Field Derivation for $Na_2SiF_6$, $Na_2GeF_6$, and $Na_3AlF_6$.** $Na_2SiF_6$,[19] $Na_2GeF_6$[20], and $Na_3AlF_6$ (cryolite)[21] are

(34) Sanders, M. J.; Leslie, M.; Catlow, C. R. A. *J. Chem. Soc. Chem. Commun.* **1984**, 1271.
(35) Jackson, R. A.; Catlow, C. R. A. *Mol. Simul.* **1988**, *1*, 207.
(36) Gale, J. D.; Henson, N. J. *J. Chem. Soc., Faraday Trans.* **1994**, *90*, 3175.
(37) Gale, J. D. *J. Phys. Chem. B* **1998**, *102*, 5423.
(38) Caullet, P.; Guth, J. L.; Hazm, J.; Lamblin, J. M. *Eur. J. Solid State Inorg. Chem.* **1991**, *28*, 345.
(39) Wagner, P.; Zones, S. I.; Davis, M. E.; Medrud, R. C. *Angew. Chem., Int. Ed.* **1999**, *38*, 1269.
(40) Harrison, R.; Nichols, J.; Straatsma, T.; Dupuis, M.; Bylaska, E.; Fann, G.; Windus, T.; Apra, E.; Anchell, J.; Bernholdt, D.; Borowski, P.; Clark, T.; Clerc, D.; Dachsel, H.; de Jong, B.; Deegan, M.; Dyall, K.; Elwood, D.; Fruchtl, H.; Glendenning, E.; Gutowski, M.; Hess, A.; Jaffe, J.; Johnson, B.; Ju, J.; Kendall, R.; Kobayash, R.; Kutteh, R.; Lin, Z.; Littlefield, R.; Long, X.; Meng, B.; Nieplocha, J.; Niu, S.; Rosing, M.; Sandrone, G.; Stave, M.; Taylor, H.; Thomas, G.; van Lenthe, J.; Wolinski, K.; Wong, A.; Zhang, Z. *NWChem, A Computational Chemistry Package for Parallel Computers, Version 4.0*; Pacific Northwest National Laboratory: Richland, WA, 2000.

**Table 2. Selected Structural Parameters of $Na_2SiF_6$, $Na_2GeF_6$, and $Na_3AlF_6$ Taken from References 19, 20, and 21, Respectively[a]**

| | initial | optimized | number |
|---|---|---|---|
| $Na_2SiF_6$ (space group *P*321, No. 150) | | | |
| a | 8.8590 | 8.8859 | |
| b | 8.8590 | 8.8859 | |
| c | 5.0380 | 5.0577 | |
| Na1−F | 2.2972 | 2.2693 | 2 |
| | 2.3567 | 2.3481 | 2 |
| | 2.4526 | 2.5082 | 2 |
| Na2−F | 2.1851 | 2.1556 | 2 |
| | 2.3076 | 2.3289 | 2 |
| | 2.3125 | 2.3485 | 2 |
| Si1−F | 1.6741 | 1.7048 | 6 |
| Si2−F | 1.6822 | 1.7077 | 3 |
| | 1.6951 | 1.7089 | 3 |
| $Na_2GeF_6$ (space group *P*321, No. 150) | | | |
| a | 9.0576 | 9.0501 | |
| b | 9.0576 | 9.0501 | |
| c | 5.1071 | 5.0946 | |
| Na1−F | 2.2231 | 2.1668 | 2 |
| | 2.3377 | 2.3392 | 2 |
| | 2.3708 | 2.3709 | 2 |
| Na2−F | 2.2807 | 2.2746 | 2 |
| | 2.3238 | 2.3599 | 2 |
| | 2.4247 | 2.5208 | 2 |
| Ge1−F | 1.7830 | 1.7717 | 6 |
| Ge2−F | 1.7841 | 1.7757 | 3 |
| | 1.8040 | 1.7767 | 3 |
| $Na_3AlF_6$ (space group $P2_1/n$, No. 14) | | | |
| a | 5.4058 | 5.4166 | |
| b | 5.5926 | 5.5408 | |
| c | 7.7699 | 7.7764 | |
| $\beta$ | 90.195 | 90.200 | |
| Na1−F | 2.2174 | 2.1882 | 2 |
| | 2.2568 | 2.2727 | 2 |
| | 2.2649 | 2.2752 | 2 |
| Na2−F | 2.2812 | 2.2521 | 1 |
| | 2.3245 | 2.2678 | 1 |
| | 2.3461 | 2.3030 | 1 |
| | 2.3609 | 2.3454 | 1 |
| | 2.5679 | 2.5666 | 1 |
| | 2.6435 | 2.6847 | 1 |
| | 2.6881 | 2.6915 | 1 |
| Al−F | 1.8053 | 1.8137 | 2 |
| | 1.8110 | 1.8211 | 2 |
| | 1.8210 | 1.8221 | 2 |

[a] The optimized values are obtained with our new force field (parameters in Table 3). All distances are in Å and angles are in degrees.

the compounds chosen to parametrize the Si−F, Ge−F, and Al−F interactions, and they all contain $TF_6$ octahedra (T = Si, Ge, Al). Synthetic cryolite is a complex fluoride with the perovskite structure where Al atoms occupy octahedral sites and Na atoms occupy both octahedral ($^1/_3$) and 12 coordinate sites ($^2/_3$). The cell parameters and selected interatomic distances are shown in Table 2.

For the three fluoro compounds a concurrent fit was performed. Apart from the T−F (T = Si, Ge, Al), Na−F, and F−F interactions, the fluoride polarizability was also parametrized through the core−shell charge split and force constant based on these three systems. The final parameters obtained are listed in Table 3. The quality of a fit can be measured by the sum of the squares of the differences between the experimental and calculated values for the observables, and here a value of 15.5 was obtained, based on the default weightings, which is low enough to be considered a good quality fit. Furthermore, the comparison between the original and optimized structures (Table 2) shows excellent agreement for a transferable force field. Here we are primarily interested in the T−F distances since these will be the most significant structural quantities for the better understanding of the role of fluoride in the synthesis of zeolites. All optimized bond lengths are overestimated, with the errors being 0.03 Å for Si−F in $Na_2SiF_6$, less than 0.03 Å for Ge−F in $Na_2GeF_6$, and less than 0.02 Å for Al−F distances in $Na_3AlF_6$, which represents satisfactory overall agreement. In addition to the errors in the parametrization of the hexafluoro compounds themselves, we have to take into account that a second source of error will arise from the transfer of this force field to the slightly different fluoride environment of the zeolite. Finally, a third source of error will be the quality of the ulterior O−F fit, although we will explain later how this part will tend to compensate the previous two deficiencies.

A further issue related to the transferring of the fit from the hexafluoro compounds to the fluoride-containing zeolites is the fact that there may be a change in $F^-$ polarizability between the two environments. This is quite difficult to estimate, and it is widely known that anions are much more sensitive to changes in polarizability than cations in different crystals.[41] From an intuitive point of view, fluoride anions should be more covalent in hexafluoro compounds than in zeolites because in the latter they are less bonded to the framework atoms. The reason for this is the effect of the zeolite framework oxygens, which produce both electrostatic and short-range repulsive effects thus making, in principle, the T−F bond in zeolites larger than the T−F bond in the corresponding hexafluoride compound. Thus, it is expected that Si−F bonds in zeolites will not be shorter than 1.68 Å (which is the shortest value in $Na_2SiF_6$ as seen from Table 2). On the other hand, experimental Si−F distances in zeolites are very much environment dependent, and while in some cases Si−F distances shorter than 1.80 Å do exist, this indicates the existence of a true covalent Si−F bond. In other cases Si−F distances as large as 2.6 Å appear, in particular when $F^-$ is located inside a D4R cage, and this points to a clearly more marked ionic character. This undoubtedly indicates that slightly different polarizabilities should be employed for $F^-$ in both extreme cases in zeolites, and therefore a source of inaccuracy may come from the fact that our model assigns a fixed polarizability to the fluoride anion. However, one of the benefits of the shell model approach is that the polarizability is intrinsically coupled to the local environment. Consequently, the model may indeed already capture the major part of the variation. Furthermore, any deficiency will be partly compensated during the derivation of the O−F potential based on the true zeolitic fluoride environment.

Although, as discussed above, the polarizability of anions is certainly sensitive to changes in the crystalline environment, in the present case the changes are not so crucial as to have a marked influence on the chemical behavior of the fluoride anion, and so the polarizability of fluoride obtained from the hexafluoride fit (Table 3) is perfectly valid for $F^-$ zeolites. A relative comparison between our values for the oxygen and fluorine anion polarizabilities is quite similar to

(41) Fowler, P. W.; Madden, P. A. *Phys. Rev. B* **1984**, *29*, 1035.

**Table 3. Interatomic Potential Parameters for Si/Ge/Al Zeolites Containing Fluoride Anions**

Atomic Charges (a.u.)

| atom | core | shell | reference |
|---|---|---|---|
| Si | 4.0 | | 22 |
| Ge | 4.0 | | 22 |
| Al | 3.0 | | this work |
| Na | 1.0 | | this work |
| F | 0.56 | −1.56 | this work |
| O in Ge−O−Ge | 1.733957 | −3.733957 | 22 |
| O in Si−O−Si, Si−O−Al, Al−O−Al | 0.870733 | −2.870733 | 22 |
| O in Ge−O−Si, Ge−O−Al | 1.330431 | −3.330431 | 22 |

Buckingham

| *i* | *j* | $A_{ij}$(eV) | $\rho_{ij}$(Å) | $C_{ij}$(eVÅ$^6$) | reference |
|---|---|---|---|---|---|
| O shell | O shell | 22764.0 | 0.149000 | 10.937044 | 22 |
| Si core | O shell | 1315.2478 | 0.317759 | 10.141118 | 22 |
| Ge core | O shell | 1497.3996 | 0.325646 | 16.808599 | 22 |
| Si core | F shell | 976.82887 | 0.282000 | 0.000000 | this work |
| Ge core | F shell | 681.47288 | 0.320000 | 0.000000 | this work |
| Al core | F shell | 801.43030 | 0.292730 | 0.000000 | this work |
| F shell | F shell | 540.39761 | 0.262490 | 0.000000 | this work |
| Al core | O shell | 1185.0000 | 0.317759 | 10.141118 | this work |
| Na core | O shell | 2110.3552 | 0.284064 | 0.000000 | this work |
| O shell | F shell | 1675.0000 | 0.268000 | 0.000000 | this work |

Three-Body

| *i* | *j* | *k* | $k_{ijk}$(eV rad$^{-2}$) | $\theta_0$(deg) | reference |
|---|---|---|---|---|---|
| O shell | Si core | O shell | 1.2614 | 109.47 | 22 |
| O shell | Al core | O shell | 1.2614 | 109.47 | this work |

Spring[a]

| *i* | *j* | $k_{ij}^{cs}$(eVÅ$^{-2}$) | reference |
|---|---|---|---|
| O(Ge−O−Ge) core | O(Ge−O−Ge) shell | 180.31577 | 22 |
| O(Si−O−Si) core | O(Si−O−Si) shell | 75.96980 | 22 |
| O(Ge−O−Si) core | O(Ge−O−Si) shell | 128.14279 | 22 |
| O(Al−O−Si) core | O(Al−O−Si) shell | 75.96980 | this work |
| O(Al−O−Al) core | O(Al−O−Al) shell | 75.96980 | this work |
| F core | F shell | 33.452757 | this work |

[a] Atomic polarizabilities can be calculated from the equation $\alpha = y^2/k$, where $y$ is the shell charge and $k$ is the spring constant.

that obtained from ab initio quantum chemical methods that take into account correlation effects by means of the coupled cluster scheme.[42] In this quantum mechanical study a ratio of $\alpha(O)/\alpha(F) = 1.80$ (where $\alpha$ is the polarizability) was obtained (taken from CaO, MgO and NaF, KF), whereas in our model a value of $\alpha(O)/\alpha(F) = 1.49$ is found. Although this reasonable agreement does not mean that our approach is as accurate as an ab initio method, we certainly believe that the $F^-$ polarizability obtained from the fit in Table 3 is transferable to the fluoride environment in zeolites.

**3.2 Force Field Derivation of the O−F Short-Range Interaction.** As already stated, the O−F interaction is not present in the hexafluoride compounds used in the previous parametrization and therefore the data for the fitting of this term have to be taken from somewhere else. The obvious choice is to derive this term from $F^-$ zeolite structures, and, for this to be possible, at least one structure is needed in which the coordinates of all atoms are known with the highest possible accuracy. The presence of $F^-$ means that the positively charged organic SDA is also present in the structure, and with the many variables that this introduces into the system this makes empirical derivation of the oxygen−fluorine interaction rather complex.

To obtain an initial starting point for the O−F interaction, a series of optimizations of the system with different sets of O−F parameters were performed. The main difference between this approach and the previously chosen relaxed fitting used above is that the process is performed manually and the assessment of quality of fit can be made through the comparison of bond lengths and overall correctness of the fluoride position, rather than through a quantitative assessment of the fractional coordinates. The initial O−F parameters were obtained by systematic variation of the Buckingham *A* term between 800 and 2000 eV, and between 0.19 and 0.30 for the $\rho$ term, which are extreme values that yield behavior in both cases that is too attractive and too repulsive, respectively. After comparison against the experimental data, a set of values was selected for refinement.

In this work, we have taken the structures of [F-DMABO]−SSZ-35[43] and [F-DABCO]−ASU-9,[16] where in both cases the zeolite structure, fluoride location, and SDA location have been reported. It should be noted that although the first material (SSZ-35) is a pure silica structure and the second one (ASU-9) is a pure germania structure, the O−F short-range parameters are the same regardless of whether the oxygen type comes from silica or germania materials. Therefore, the different oxygen types in SSZ-35 and ASU-9 do not present any problem when enforcing a common potential during the parametrization.

(42) Doll, K.; Stoll, H. *Phys. Rev. B* **1997**, *56*, 10121.

(43) Fyfe, C. A.; Brouwer, D. H.; Lewis, A. R.; Villaescusa, L. A.; Morris, R. E. *J. Am. Chem. Soc.* **2002**, *124*, 7770.

Another point to highlight is the fact that the fluoride ion occupies different environments in the SSZ-35 ($[4^15^26^2]$ cages) and ASU-9 ($[4^6]$ cages, also called D4R) materials, and that this is an advantage for the fit, in the sense that it reflects the multiplicity of environments that fluoride anions can occupy in zeolites. Hence, the fact that the O−F Buckingham term is adjusted to reproduce both structures as closely as possible, improves the transferability of the fit and makes it more suitable for application to all zeolite structures. In the first of the structures, SSZ-35, there is a real Si−F bond with a distance of about 1.74 Å,[43] whereas in the second, ASU-9, although a large Ge−F distance about 2.7 Å has been reported,[16] corresponding to fluoride anions in the middle of the D4R, some reservations about this assignment have appeared recently. It is suggested that fluoride may not be located at the center of the D4R but rather in an off-centered position.[44,45]

Given the ambiguities concerning the crystallographic location of fluoride in close contact with oxygen, such as when sited within the D4R unit in the $GeO_2$ structure ASU-9, an ab initio calculation has been used to determine the final parameters for the potential, which can then be tested on the structure of SSZ-35. To do this, the following procedure was adopted. First, the structure of ASU-9 consisting of a purely germania framework was optimized while including the presence of the template and the fluoride ions, based on the force field parameters, including an initial estimate of the O−F interaction. Subsequently the framework was held fixed and all extraframework ions, except for the fluoride ion in the D4R, were removed. This creates a system where the framework is positioned close to the as synthesized form, but without the complexity of the template being actually present. The position of the fluoride ion alone was then optimized, in the presence of a charge-neutralizing background, using periodic density functional theory. For this purpose, we have employed the SIESTA methodology,[46] in which the atoms are described using a combination of pseudopotentials and a DZP basis set, where the spatial extent of the orbitals is confined to a radius, such that the energy increases by 0.01 Ry. The calculations were performed using the GGA functional of Perdew et al.[47] with sampling of the Brillouin zone restricted to the Γ-point, and a real space mesh with an energy cutoff of 250 Ry was used as an auxiliary basis set in the determination of the Hartree and exchange-correlation potentials. The fluoride ion was minimized until all forces acting on it were less than 0.001 eV/Å.

The above ab initio calculation yielded an off-center position for the fluoride ion within the D4R unit of the ASU-9 structure. A Ge−F covalent bond with a distance of 2.16 Å was obtained from the force field optimization, which compares very well with the Ge−F distance of 2.18 Å observed in the ab initio structure, both results indicating the presence of a pentacoordinated Ge. Because of this lower symmetry, there is sufficient information to refine the O−F Buckingham potential such that the equivalent force field calculation yields the same minimum. The final parameters for the O−F interaction determined from this procedure are given in Table 3. The structural features of the ASU-9 structure, as optimized with this force field are shown in Table 4, and the full structural characterization from the force field as well as the ab initio calculations are given as Supporting Information.

**Table 4. Selected Structural Parameters of ASU-9 (AST) Optimized with the Force Field in Table 3[a,b]**

| T−F-labels | | T−F | number |
|---|---|---|---|
| Ge1 | F | 2.159 | 1 |
| Ge1 | F | 2.160 | 1 |
| **T−O-labels** | | **T−O** | **number** |
| Ge1 | O1 | 1.716 | 14 |
| Ge1 | O2 | 1.722 | 12 |
| Ge1 | O3 | 1.724 | 24 |
| Ge1 | O2F | 1.712 | 2 |
| Ge1 | O3F | 1.722 | 4 |
| Ge1F | O1F | 1.779 | 2 |
| Ge1F | O2F | 1.740 | 2 |
| Ge1F | O3F | 1.740 | 4 |
| Ge2 | O1 | 1.726 | 14 |
| Ge2 | O1F | 1.685 | 2 |

| T−O−T-labels | | | T−O−T | number |
|---|---|---|---|---|
| Ge1 | O1 | Ge2 | 135.11 | 14 |
| Ge1 | O2 | Ge1 | 139.08 | 6 |
| Ge1 | O3 | Ge1 | 137.86 | 12 |
| Ge1F | O1F | Ge2 | 133.09 | 2 |
| Ge1F | O2F | Ge1 | 128.87 | 2 |
| Ge1F | O3F | Ge1 | 127.17 | 4 |

| O−T−O-labels | | | O−T−O | number |
|---|---|---|---|---|
| O1F | Ge1F | O2F | 96.88 | 2 |
| O1F | Ge1F | O3F | 96.58 | 4 |
| O2F | Ge1F | O3F | 116.45 | 4 |
| O3F | Ge1F | O3F | 121.74 | 2 |

[a] Two molecules of SDA are present in the $Ge_{20}O_{40}$ unit cell and two fluoride anions, located in $[4^6]$ cages (D4R). The coordinates of the optimized cell, with the SDA and fluoride anions, are in the Supporting Information (Table S1a). Germanium and oxygen atoms are labeled as in ref 16. All distances are in Å and angles are in degrees. [b] ASU-9, two fluorides, two DABCO cations: see Table S1a in Supporting Information for the unit cell coordinates. Cell parameters: $a = 9.3082$ Å, $b = 9.0779$ Å, $c = 14.3443$ Å, $\alpha = 91.21°$, $\beta = 90.37°$, $\gamma = 88.83°$.

On the basis of this force field, a first test was performed on the structure of SSZ-35, which is well characterized experimentally, and the agreement between the force field optimized and the experimental structure is quite remarkable. Selected structural features of the optimized [F-DMABO]−SSZ-35 structure are given in Table 5, where it can be seen that values close to those experimentally determined are obtained. For the Si−F covalent bonds, the calculated values (1.756−1.790 Å) are within 0.05 Å of the experimental value (1.745 Å). For the $Si_F$−O distances (where $Si_F$ is the silicon bonded to the fluoride ion) also a remarkable agreement, within 0.04 Å, is obtained; except in the Si4F−O5F distance in which a larger discrepancy (within 0.08 Å) is found. Regarding the $Si_F$−O−Si angles, a very remarkable agreement, less than 5°, is observed. Finally, the O−$Si_F$−O angles are less accurately reproduced (two of them disagree in nearly 10°, although most of them are within 5°) but still the trends

(44) Villaescusa, L. A.; Lightfoot, P.; Morris, R. E. *Chem. Commun.* **2002**, 2220.
(45) Wang, Y.; Song, J.; Gies, H. *Solid State Sci.* **2003**, *5*, 1421.
(46) Soler, J. M.; Artacho, E.; Gale, J. D.; García, A.; Junquera, J.; Ordejón, P.; Sánchez-Portal, D. *J. Phys. Condens. Mater.* **2002**, *14*, 2745.
(47) Perdew, J. P.; Burke, K.; Ernzerhof, M. *Phys. Rev. Lett.* **1996**, *77*, 3865.

**Table 5. Selected Structural Parameters of SSZ-35 (STF) Optimized with the Force Field Given in Table 3, Including Experimental Values from Reference 43[a,b]**

| | | | dist-1 | dist-2 | exp | |
|---|---|---|---|---|---|---|
| T−F-labels | | | T−F | | | number |
| Si4F | F | | 1.765 | 1.779 | 1.745 | 1 |
| Si4F | F | | 1.756 | 1.790 | 1.745 | 1 |
| T−O-labels | | | T−O | | | number |
| Si4F | O5F | | 1.686 | 1.699 | 1.761 | 2 |
| Si4F | O6F | | 1.709 | 1.680 | 1.665 | 2 |
| Si4F | O7F | | 1.665 | 1.665 | 1.633 | 2 |
| Si4F | O8F | | 1.675 | 1.669 | 1.651 | 2 |
| T−O−T-labels | | | T−O−T | | | number |
| Si4F | O5F | Si2 | 135.28 | 132.96 | 135.20 | 2 |
| Si4F | O6F | Si1 | 129.83 | 130.73 | 130.09 | 2 |
| Si4F | O7F | Si7 | 146.26 | 141.95 | 147.65 | 2 |
| Si4F | O8F | Si5 | 140.26 | 139.62 | 143.97 | 2 |
| O−T−O-labels | | | O−T−O | | | number |
| O5F | Si4F | O6F | 85.083 | 87.78 | 90.15 | 2 |
| O5F | Si4F | O7F | 89.154 | 89.38 | 93.04 | 2 |
| O5F | Si4F | O8F | 90.402 | 88.07 | 90.75 | 2 |
| O6F | Si4F | O7F | 123.930 | 122.04 | 111.98 | 2 |
| O6F | Si4F | O8F | 123.460 | 122.27 | 119.34 | 2 |
| O7F | Si4F | O8F | 113.308 | 115.36 | 124.89 | 2 |

[a] Two molecules of SDA are present in the $Si_{32}O_{64}$ unit cell and two fluoride anions, located in [$4^1 5^2 6^2$] cages. Four such cages exist and only two are occupied by fluoride. Depending on the fluoride occupancy, a different SDA distribution is followed as indicated in the Supporting Information (Table S2a and S2b). Silicon and oxygen atoms are labeled as in ref 43, except for the fact that an "F" has been added, for the sake of clarity, to the atoms belonging to the pentacoordinated Si,[$SiO_{4/2}F$]$^-$ unit. All distances are in Å and angles are in degrees. [b] SSZ-35, two fluorides, two DMABO cations. Distribution-1, distribution-2, and experimental values are indicated under columns dist-1, dist-2, and exp, respectively. The cell parameters are $a = 7.3876$ Å, $b = 17.8817$ Å, $c = 13.9589$ Å, $\alpha = 90.10^\circ$, $\beta = 99.63^\circ$, $\gamma = 91.57^\circ$ (distribution-1, with unit cell coordinates in Table S2a); $a = 7.3949$ Å, $b = 17.8298$ Å, $c = 13.9351$ Å, $\alpha = 89.73^\circ$, $\beta = 99.22^\circ$, $\gamma = 88.07^\circ$ (distribution-2, with unit cell coordinates in Table S2b); $a = 7.4573$ Å, $b = 18.0966$ Å, $c = 14.0233$ Å, $\alpha = 90.00^\circ$, $\beta = 99.25^\circ$, $\gamma = 90.00^\circ$ (experimental).

are quite consistent and they are within what is expected in a trigonal bipyramid geometry as it corresponds to the pentacoordinated $Si_F$ atom. The full, optimized, structural details are provided as Supporting Information. We further note that because of the general nature of the short-range O−F interaction, regardless of the oxygen framework type, this term is of general use for oxygen and fluorine in zeolites and zeotypes.

**3.3 Force Field Derivation for Zeolites with Si/Ge/Al Framework Composition.** The present force field is an extension of our previous Si/Ge force field,[22] and the parameters relating to the simulation of Si/Ge zeolites have remained unchanged. To be able to model materials containing any amount and ordering of Si/Ge/Al as framework atoms, as well as $F^-$ and any organic SDA, this only now requires the inclusion of the Al−O short-range term to the force field derived so far. To perform the fit, we have chosen a zeolite structure with Si/Al = 1,[23] since we believe this allows for a better description of the contribution of Al to the framework structure. The LTA structure by Pluth and Smith[23] is well characterized by XRD, and the fact that Si/Al = 1, in combination with Lowenstein's rule,[24] ensures a strict ordering of Si−Al with no Si−O−Si or Al−O−Al bonds present. Although the Buckingham Al−O term contains three parameters, $A$, $\rho$, and $C$ (see eq 2), the latter two may be fixed to the same values as for Si−O and we can obtain the fit by only changing the value of the $A$ parameter. Inclusion of the $\rho$ parameter in the fit yields little benefit since there is no curvature information available to deconvolute the contribution of the two repulsive parameters. Furthermore, the three-body term for O−Al−O angles has been kept fixed to the same value as for O−Si−O since both atoms (Si and Al) are expected to behave similarly regarding the tetrahedral stiffness. During the fit, which was performed within the $Fm\bar{3}c$ (No. 226) space group, not only the crystallographic cell parameters and the atomic coordinates, but also the bond distances and angles, were monitored to minimize the differences between the original structure and the optimized one obtained after the fit. With regard to the sodium cation distribution, three sodium sites are present, Na1, Na2, and Na3, and their relative occupation was chosen to be as similar as possible to the experimentally reported values.[23] However, the two conditions [Na] = [Al] (electroneutrality) and [Si] = [Al] (Si/Al = 1), are not completely followed in the XRD refinement. As a result, the cation position occupancies chosen were 0.972, 0.242, and 0.110 (compared to the experimentally reported values of 0.972, 0.242, and 0.066) for Na1, Na2, and Na3, respectively. The experiments correspond to the refined cell $Na_{91.78}Si_{96}Al_{96}O_{384}$,[23] whereas our asymmetric unit with cubic symmetry corresponds to the cell $Na_{96}Si_{96}Al_{96}O_{384}$. The final value of 1185 for the $A$ parameter (see Table 3) was chosen, and the final test of the accuracy of the fit was performed through an optimization of the full unit cell $Na_{96}Si_{96}Al_{96}O_{384}$, without symmetry constraints. Here the numbers of sodium cations with respect to the total number of sites were Na1 = 60/64, Na2 = 24/96, and Na3 = 12/96. This gives a total occupancy very close to experiment, and the cations were also located according to the criteria that the cations are as far away as possible from each other while being as close as possible to the Al framework atoms. The final optimized LTA structural parameters, bond distances, and angles are given in Table 6, where a comparison with the experimental LTA structure is provided. Calculated and experimental T−O (T = Si,Al) and Si−Al distances compare within 0.02 Å, $Si_1-O_2-Al_1$, $Si_1-O_3-Al_1$, and $Si_1-O_1-Al_1$ angles are within 5°, 3°, and 8°, respectively, and O−T−O angles are within 2° except in the case of $O_2-Al_1-O_3$ and $O_1-Al_1-O_3$, whose errors are about 6°. Overall, it can be seen that the agreement is very good and thus that the force field is definitely satisfactory. The optimized full cell coordinates of the LTA are given as Supporting Information.

**3.4 Force Field Testing with the SSZ-44 Structure.** SSZ-44 (SFF in ref 48, see Figure 1) is a structure related to SSZ-35 (STF in ref 48) and both possess an unusual one-dimensional straight channel system with a pore diameter that alternates between a 10MR and a contorted 18MR. The cage structures differ, as do the channel systems, but both

(48) Baerlocher, Ch.; Meier, W. M.; Olson, D. H. *Atlas of Zeolite Structure Types, 5th revised ed.*; Elsevier: Amsterdam, The Netherlands, 2001 (http://www.iza-structure.org).

**Table 6. Selected Structural Parameters of Na−A (LTA) Optimized with the Force Field in Table 3[a,b]**

| T−O-labels | | exp T−O | calc T−O | number |
|---|---|---|---|---|
| Si1 | O2 | 1.586 | 1.609 | 96 |
| Al1 | O2 | 1.717 | 1.718 | 96 |
| Si1 | O3 | 1.604 | 1.619 | 192 |
| Al1 | O3 | 1.741 | 1.734 | 192 |
| Si1 | O1 | 1.595 | 1.620 | 96 |
| Al1 | O1 | 1.723 | 1.739 | 96 |

| T−T-labels | | T−T | | number |
|---|---|---|---|---|
| Si1 | Al1 | 3.198 | 3.213 | 384 |

| T−O−T-labels | | | T−O−T | | number |
|---|---|---|---|---|---|
| Si1 | O2 | Al1 | 164.72 | 170.35 | 96 |
| Si1 | O3 | Al1 | 144.81 | 147.94 | 192 |
| Si1 | O1 | Al1 | 142.25 | 134.66 | 96 |

| O−T−O-labels | | | O−T−O | | number |
|---|---|---|---|---|---|
| O1 | Si1 | O2 | 108.63 | 108.69 | 96 |
| O1 | Si1 | O3 | 111.35 | 110.87 | 192 |
| O2 | Si1 | O3 | 107.14 | 107.17 | 192 |
| O3 | Si1 | O3 | 111.11 | 111.71 | 96 |
| O2 | Al1 | O1 | 107.97 | 107.62 | 96 |
| O2 | Al1 | O3 | 105.94 | 111.78 | 192 |
| O1 | Al1 | O3 | 112.38 | 106.05 | 192 |
| O3 | Al1 | O3 | 111.86 | 112.77 | 96 |

| T-label | O−T−O | | number |
|---|---|---|---|
| Si1 | 109.45 | 109.41 | 576 |
| Al1 | 109.41 | 109.34 | 576 |

[a] Na-A, labeled as in ref 23. The unit cell is $Na_{96}Si_{96}Al_{96}O_{192}$ and an ordered Si−Al distribution is followed. Three cation sites (Na1, Na2, Na3) are present with number of sites 64, 96, and 96, respectively, and the occupations in the unit cell are 60, 24, and 12, respectively, following the experimental XRD structure in ref 23. The coordinates of the optimized cell are given in the Supporting Information (Table S3). Sodium, silicon, aluminum, and oxygen atoms are labeled as in ref 23. All distances are in Å and angles are in degrees. [b] Calculated and experimental values are indicated under columns exp and calc, respectively. The cell parameters are $a = 24.5550$ Å, $b = 24.5550$ Å, $c = 24.5550$ Å (experimental, where the space group is $Fm\bar{3}c$, No. 226); $a = 24.6379$ Å, $b = 24.6684$ Å, $c = 24.6963$ Å, $\alpha = 90.03°$, $\beta = 89.97°$, $\gamma = 90.04°$ (calculated, with unit cell coordinates in Table S3).

materials have in common a layerlike unit which, through the formation of different linkages between the layers, produce different microporous systems.[39] Although the effect of the different organic SDAs used in the synthesis may be responsible for the change in the stacking in the final structure, this effect is not entirely understood. A better understanding of the systems might make it feasible to control the stacking percentage of the two end members in the final material obtained. Although SSZ-44 was originally synthesized in hydroxide media with *N*,*N*-diethyl-2,6-cis-dimethylpiperidinium, only the calcined structure has been solved by synchrotron powder XRD.[39] Recently, SSZ-44 was obtained in fluoride media by using the same SDA and, although the crystals obtained are not of sufficient quality to solve the structure by single-crystal XRD methods, a very accurate $^{19}F$ NMR study has been performed to characterize the local structure of the $[SiO_{4/2}F]^-$ units.[49] The reason we have chosen the unsolved [F-DECDMP]−SSZ-44 structure

(49) Darton, R. J.; Brouwer, D. H.; Fyfe, C. A.; Villaescusa, L. A.; Morris, R. E. *Chem. Mater.* **2004**, *16*, 600.

**Table 7. Selected Structural Parameters of SSZ-44 (SFF) Optimized with the Force Field in Table 3[a]**

Distribution-1[b]

| T−F-labels | | T−F | number |
|---|---|---|---|
| Si3 | F | 1.772 | 1 |
| Si3 | F | 1.775 | 1 |

| T−O-labels | | T−O | number |
|---|---|---|---|
| Si3F | O6F | 1.677 | 2 |
| Si3F | O8F | 1.727 | 2 |
| Si3F | O9F | 1.690 | 2 |
| Si3F | O10F | 1.652 | 2 |

| T−O−T-labels | | | T−O−T | number |
|---|---|---|---|---|
| Si3F | O6F | Si2 | 137.62 | 2 |
| Si3F | O8F | Si3 | 136.72 | 2 |
| Si3F | O9F | Si4 | 129.15 | 2 |
| Si3F | O10F | Si5 | 149.60 | 2 |

| O−T−O-labels | | | O−T−O | number |
|---|---|---|---|---|
| O6F | Si3F | O8F | 89.62 | 2 |
| O6F | Si3F | O9F | 121.67 | 2 |
| O6F | Si3F | O10F | 117.33 | 2 |
| O8F | Si3F | O9F | 88.84 | 2 |
| O8F | Si3F | O10F | 85.81 | 2 |
| O9F | Si3F | O10F | 120.67 | 2 |

Distribution-2

| T−F-labels | | T−F | number |
|---|---|---|---|
| Si4F | F | 1.773 | 1 |
| Si5F | F | 1.777 | 1 |

| T−O-labels | | T−O | number |
|---|---|---|---|
| Si4F | O2F | 1.673 | 1 |
| Si4F | O9F | 1.727 | 1 |
| Si4F | O11F | 1.656 | 1 |
| Si4F | O12F | 1.698 | 1 |
| Si5F | O7F | 1.662 | 1 |
| Si5F | O10F | 1.676 | 1 |
| Si5F | O13F | 1.668 | 1 |
| Si5F | O14F | 1.730 | 1 |

| T−O−T-labels | | | T−O−T | number |
|---|---|---|---|---|
| Si4F | O2F | Si1 | 146.44 | 1 |
| Si4F | O9F | Si3 | 127.05 | 1 |
| Si4F | O11F | Si8 | 140.96 | 1 |
| Si4F | O12F | Si8 | 138.33 | 1 |
| Si5F | O7F | Si2 | 133.67 | 1 |
| Si5F | O10F | Si3 | 136.05 | 1 |
| Si5F | O13F | Si7 | 126.88 | 1 |
| Si5F | O14F | Si5 | 129.59 | 1 |

| O−T−O-labels | | | O−T−O | number |
|---|---|---|---|---|
| O2F | Si4F | O9F | 124.93 | 1 |
| O2F | Si4F | O11F | 118.47 | 1 |
| O2F | Si4F | O12F | 89.72 | 1 |
| O9F | Si4F | O11F | 116.56 | 1 |
| O9F | Si4F | O12F | 88.09 | 1 |
| O11F | Si4F | O12F | 90.04 | 1 |
| O7F | Si5F | O10F | 116.28 | 1 |
| O7F | Si5F | O13F | 117.10 | 1 |
| O7F | Si5F | O14F | 88.67 | 1 |
| O10F | Si5F | O13F | 123.54 | 1 |
| O10F | Si5F | O14F | 84.043 | 1 |
| O13F | Si5F | O14F | 89.610 | 1 |

[a] Two molecules of SDA are present in the $Si_{32}O_{64}$ unit cell and two fluoride anions, located in $[4^15^26^2]$ cages. Four such cages exist and only two are F-occupied. Different fluoride locations in the cages have been tested and the coordinates of all atoms are given as Supporting Information (Table S4a and S4b). Silicon and oxygen atoms are labeled as in ref 39, except for the fact that an "F" has been added, for the sake of clarity, to the atoms belonging to the pentacoordinated Si, $[SiO_{4/2}F]^-$ unit. All distances are in Å and angles are in degrees. [b] SSZ-44, two fluorides, two DECDMP cations, distribution-1 (see Table S4a in Supporting Information for the unit cell coordinates). Cell parameters: $a = 11.4438$ Å, $b = 21.6580$ Å, $c = 7.4192$ Å, $\alpha = 90.21°$, $\beta = 94.97°$, $\gamma = 90.70°$. [c] SSZ-44, two fluorides, two DECDMP cations, distribution-2 (see Table S4b in Supporting Information for the unit cell coordinates). Cell parameters: $a = 11.3818$ Å, $b = 21.8887$ Å, $c = 7.4014$ Å, $\alpha = 89.70°$, $\beta = 94.97°$, $\gamma = 89.62°$.

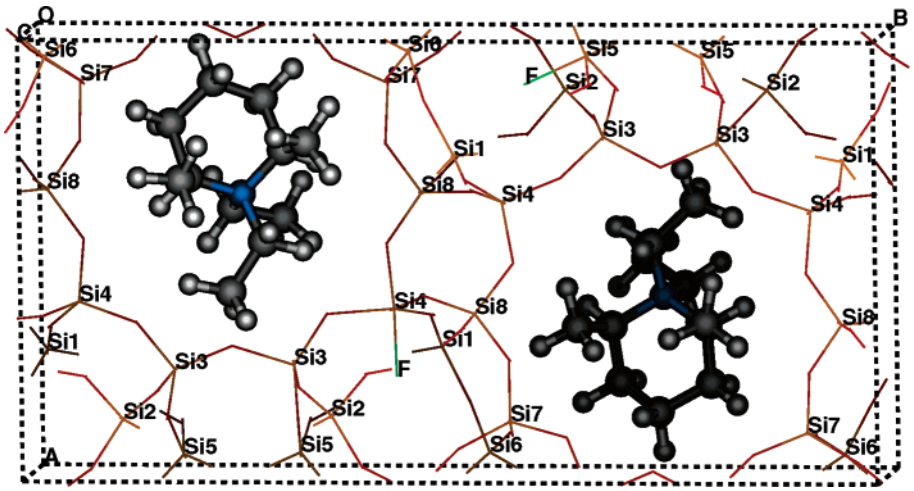


**Figure 1.** Unit cell of SSZ-44 (SFF) structure with two molecules of $DECDMP^+$ and two $F^-$ anions located each in a $[4^15^26^2]$ cavity. Four cavities are present in the unit cell, which corresponds to a 50% $F^-$ occupancy. Silicon atoms are labeled as in ref 39. This $F^-$ occupation corresponds to the unit cell described in Table S4b of Supporting Information, and the Si−F distances are Si5−F = 1.777 Å, Si4−F = 1.773 Å.

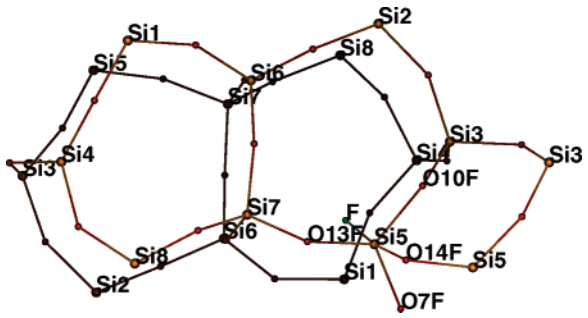


**Figure 2.** Double $[4^15^26^2]$ cavity in SSZ-44 with the $F^-$ attached to Si5. This does correspond to the unit cell of Figure 1. Silicon atoms are labeled as in ref 39. This $F^-$ occupation corresponds to the unit cell described in Table S4b of Supporting Information, and the Si−F distance is Si5−F = 1.777 Å. It can be seen that the pentacoordinated Si exhibits a trigonal bipyramid geometry. The corresponding bond distances and angles are listed in Table 7 (distribution-2).

to test our force field is because there are very few structures where the local structure of the $[SiO_{4/2}F]^-$ units is actually well characterized enough to compare against without averaging over $[SiO_{4/2}]$ units in the fluoride unoccupied cages. One such structure that has been solved is SSZ-35,[43] which has been used for testing the present force field, and we believe that, to date, it is the only one solved (without averaging over occupied and unoccupied cages) with $F^-$ in non-D4R cages.

The study of SFF indicates a Si−F distance of 1.79 Å.[49] Our optimization has been performed by taking the coordinates of the calcined SSZ-44 structure,[39] then introducing both the organic SDA[39,49] and the fluoride anions, as per the original reference.[49] The resulting fully minimized structure is shown in Figure 1 and in Table 7. From this we have obtained a favorable location for $F^-$ in the $[4^15^26^2]$ cages of SFF and two low energy distributions of sites have been characterized (Table 7). In the first distribution, the two fluoride anions present in the unit cell are both attached to Si3 with optimized covalent distances of 1.772 and 1.775 Å, respectively, whereas in the second distribution they are attached to Si4 and Si5 at distances of 1.773 and 1.777 Å. The first distribution is more stable by 21.6 kJ/mol per unit cell, but both of them are close enough in stability so as to have the potential to be experimentally observable. Of course, other distributions are also possible, and not only the two reported here. An interesting point here is the fact that the vertex symbols (see Supporting Information), which have been calculated with the zeoTsites software,[50] for the different tetrahedral positions in SSZ-44 are the same for Si3, Si4, and Si5. Thus, there may be a link between the topological nature of the framework site and its ability to coordinate fluoride in a stable fashion. The fact that these positions are linked to a 4MR helps to confirm the hypothesis that $F^-$ tends to associate with Si in 4MR.[17] The analysis of the geometry indicates that a pentacoordinated Si appears due to the formation of the Si−F bond, and the results in Table 7, as well as the cavity aspect (Figure 2), demonstrate that a trigonal bipyramid geometry is exhibited.

**3.5 Force Field Testing with $F^-$ Vibrations in Octadecasil Zeolite.** The present force field has been parametrized mainly against structural data. However, it can also be used not only to reproduce structural features of zeotypes, but also dynamical features such as vibrational properties. A recent infrared study of octadecasil synthesized in fluoride media has been carried out.[51] Vibrational spectroscopy can give useful information when localized modes are present, and, in particular, we are here interested in modes associated with fluoride anions, which, from an experimental viewpoint, can be traced by comparing the infrared spectra of the as-synthesized (with fluoride) and the calcined (without fluoride) octadecasil structures. Although some assignments remain controversial, it has been established[51] that $F^-$ occluded in the D4Rs of octadecasil leads to the presence of three harmonic modes near 122 $cm^{-1}$. Our calculations start with the octadecasil unit cell ($Si_{20}O_{40}$) in which two molecules of the experimentally used SDA (*N*,*N*,*N*-trimethyl-tert-butylammonium) have been optimized within the microporous space of the zeolite, with two fluoride anions located inside the D4Rs (the final atomic coordinates and cell parameters are given as Supporting Information). The vibrational normal modes, as well as the atomic projected density of states, have been calculated for this optimized

(50) Sastre, G.; Gale, J. D. *Microporous Mesoporous Mater.* **2001**, *43*, 27.
(51) Villaescusa, L.; Marquez, F. M.; Zicovich-Wilson, C. M.; Camblor, M. A. *J. Phys. Chem. B* **2002**, *106*, 2796.

system. The dominant contribution of $F^-$ to the density of states is found in three vibrational modes at 120.4, 122.5, and 123.9 $cm^{-1}$ which is in excellent agreement with the 122 $cm^{-1}$ value above assigned from quantum chemical calculations of the $F^-$ motion inside the D4R of the octadecasil structure.

## 4. Conclusions

A new force field has been derived that is able to model the location and behavior of $F^-$ in Si/Ge/Al zeolites. The potential model can also be used when $F^-$ is not present in the system, and therefore it is the first force field available that allows the simulation of Si/Ge/Al zeolites. The location and energetics of $F^-$ in zeolites is of interest in determining the role played by fluoride ions in the synthesis and stabilization of zeolite structures—a purpose for which the newly parametrized force field is designed. The lack of experimental data for this type of system makes computer simulation of particular interest when used as a predictive tool to identify the location of $F^-$ in zeolites. Furthermore, the effect of chemical composition encompassing the full range of possible Si/Al/Ge distributions can be studied with the present force field. The resulting parameters have been successfully tested for the SSZ-44 structure. A pentacoordinated Si in a $SiO_{4/2}F$ environment with a trigonal bipyramid geometry is predicted to occur based on full energy minimization of the system, including the template, which resembles configurations already found in other zeolitic materials. The Si−F distances are found to lie within the range of 1.77−1.78 Å in the simulation, which is in excellent agreement with the experimental range of 1.72−1.79 Å as found by $^{19}F$ NMR.

**Acknowledgment.** G.S. thanks Ministerio de Ciencia y Tecnologia (project MAT2003-07769-C02-01) for financial support, the ITQ for funding a stay in Perth, and Centro de Proceso de Datos (Universidad Politecnica de Valencia) for the use of their computational facilities. The High Performance Computational Chemistry Group from Pacific Northwest National Laboratory (Richland, WA) is acknowledged for making available NWChem version 4.0, a computational chemistry package for parallel computers. Prof. R. E. Morris and Dr. L. A. Villaescusa are acknowledged for useful comments. J.D.G. thanks the Government of Western Australia for a Premier's Research Fellowship.

**Supporting Information Available:** Tables of cell data for the subject materials (pdf). This material is available free of charge via the Internet at http://pubs.acs.org.

CM048406O